Modelling the neural dynamics of binding in language with the Neural Blackboard Architecture

Martin Perez-Guevara[1], Marc De Kamps[2], Christophe Pallier[1],

1 Cognitive Neuroimaging Unit, CEA DSV/I2BM, INSERM, Université Paris-Sud, Université Paris-Saclay, NeuroSpin center, 91191 Gif/Yvette, France
2 Institute for Artificial Intelligence and Biological Systems. School of Computing. University of Leeds. LS2 9JT Leeds. United Kingdom

Abstract

An important challenge in neurolinguistics is to understand how variable binding is implemented in the brain. Variable binding is needed to assign words to their syntactic and semantic roles during sentence comprehension. Few attempts have been made to model complete circuits of variable binding with biological spiking neural networks. The Neural Blackboard Architecture (NBA), proposed by Van der Velde and De Kamps [1] is one of them. It was designed from the ground to solve variable binding and to address several challenges in the neural modeling of sentence processing, including the ones detailed by Jackendoff [2]. Here we expand on previous simulations of the NBA with population density techniques to obtain temporally detailed neural dynamics.

We show how different neural models constrain the circuit implementation, behavior and predictions.(CP: This sentence is vague and unclear to me. Can you make it more precise?). While Leaky-Integrate-and-Fire models have been employed before, this paper is the first attempt to extend variable binding related circuit simulations to Adaptive-Exponential models. We demonstrate that it is possible to approximate the neural dynamics of the binding of two or more words to create phrases. Moreover, we compare the simulation results with two neuroimaging experiments. First, we show that the model can qualitatively replicate recent work from Nelson et al. [3] based on intracortical recordings (EcOG), in which neural effects on phrase size and binding operations are depicted. Second, we approximate the results of an fMRI experiment which reported a sublinear increase of the amplitude of hemodynamic responses in language regions as a function of constituent size in lists of phrases [4]. In all cases we approximate the neuroimaging patterns assuming a phrase grammar theory and bottom-up parsing, but our simulations could be trivially adapted to arbitrary grammar theories and parsing schemes, which turns it into a promising hypothesis exploration device for future research in language neuroimaging.

1 Introduction

Although there is theoretical disagreement in modern linguistics about the optimal formalism to describe the internal representations of sentences in the human brain, there is a clear need for some sort of "composition" operation to process units of language [5]. This operation does not need to be exclusive to syntactic structures of language, as suggested by the 'merge' operation in the syntactocentric view of Chomsky's minimalist program [6](CP: This is an unnecessarily critical intro

(disagreement, syntctoc centric...). This is not needed: You can invert the presentaiton and first state that binding is need for all linguistics levels, whatever the adopted formalism; then only mention Chomsky's merge as the central operation in the minimalist program, if you like.), but can also expand to other stages of language processing like phonological structures, conceptual structures or even interfacing structures, as suggested by the parallel tripartite architecture of Jackendoff [7]. It is not only assumed by the notions of constituency present in the formalism of phrase structure grammars, that allow groups of words to act as one unit, but also by the alternative consideration of words relative grammatical function in dependency grammars and the more limited treelet structures proposed by Marcus [8].(CP: Treelets are actually as powerful as minimalist grammar and reach mildly context sensitive level. See Joshi TAGs. And do not attribute treelets to a chapter by Marcus. The idea is present e.g. in Joshi, Bod, ... Actually, better to not emntio treelets at all here.)

Proposing a satisfactory neural model for the "composition" operation required by language is linked to solving the binding problem initially posed within the domain of vision in neuroscience. The term binding was introduced to the neuro-scientific community by von der Malsburg [9] during the first explorations of neural phase synchronization for "variable binding", which is a term taken literally from computer science, meaning to link a data structure to a name so it can be later accessed by that name. As Jackendoff [2] explains, binding is also motivated by the empirical discovery of the distributed and segmented encoding of features along the cortex. An example of this would be color and shape in the case of vision, which are robustly integrated during perception but can be independently impaired by brain damage. Due to the combinatoric nature of sensory stimuli and in particular of language structures, simple mechanisms to link features momentarily like combination-encoding cells become unfeasible [10]. To get an idea of the massiveness of this problem we can take a simple example from Van der Velde [1]. That is, an average 17-year-old English speaker has a lexicon of more than 60.000 words, which easily allows a set of 10^{20} or more possible phrases, of 20 or less words, that can be produced and understood. Such magnitude effectively exceeds the estimated lifetime of the universe expressed in seconds, making it clear that a simple holistic encoding of sentences is not attainable in a human lifetime.

The binding problem in all its generality actually comprises four different sub problems, namely *General Coordination*, *Feature-Binding*, *Variable Binding* and the *Subjective Unity of Perception* [11]. The current work is specifically motivated by the *Variable Binding* sub-problem, which is still unsolved and is crucial to understand all cognitive faculties of symbolic thought, like language and mathematics [**?**, 12]. We provide a biologically plausible neural implementation of variable binding and validate it against experimental evidence, which so far has been difficult to attain due to the uniqueness of high-level symbolic thought in humans(CP: I find this passage a bit odd, as it seems to me that the binding problem can and has been studied in animals. Can you clarify?). This problem is illustrated by the capacity to run logical inference on data structures that encode relationships between their items. For example the sentence "*Mary owns a book*" allows to establish a relation of the type own(Mary, book) that implies owner(book, Mary), such that we can ask the question "Who owns this book?". A simple neural association(CP: Claify what is 'simple neural assocation') of the concepts *Mary*, *own* and *book* would not allow to query relations and, as pointed out before, encoding permutations is not allowed by the massiveness of the combinatoric problem.

There are two main approaches discussed in the literature to solve the binding problem. The first relies on the framework of tensor product representations and the second to connectivity based models that allow binding by process(CP: What does 'by process' mean. Is it English, or a theoretical concept?). [12] provides an in-depth

analysis of the typology of vector symbol architectures (VSA) that work with tensor operations. He shows that variouos proposal, including Synchronous Firing [13], Holographic Reduced Representations [14] and Recursive Auto-Associative Memories [15], are just particular cases with varying implementation details of his general tensor product framework. On the other hand, Van der Velde et al. [16] explains how connectivity based models are necessary to produce behavior in a sensory-motor loop and provide an internal frame of reference for the brain to implement queries.(CP: This explanation is way to quick.. You need to explain. it looks that this is something that is not handled in the VSA framework. Is it? Is it not? What is it?) He shows that models like Shruti [13], contrary to the analysis of Feldman [11], gain their capacity to implement behavior from being ultimately connectivity based(CP: Now, you should explain what "connectivity based" means.) too. Nonetheless what importantly differentiates his proposal from the tensor framework models is the idea of implementing binding by process, which consists on binding the activity of two concept encoding neural populations by controlling conditional connections between them.(CP: Question: is this a dynamic aspect which is absent (?) from VSA, allowing to bind and unbind in time?) Furthermore this idea is at the base of the Neural Blackboard Architecture proposed by Van der Velde and De Kamps [1], that claims to also solve the other challenges posed by Jackendoff to model language in the human brain.(CP: Maybe you should list these challenges. It is the second time you mention them) We will show that the proposed circuits of the architecture reveal non trivial signatures of temporally detailed neural dynamics that actually resemble results from the neuroimaging literature. Moreover, with some refinements, the produced neural signatures could be further validated directly against neural measurements from intracranial recordings, which could be the goal of future work.

1.1 Neural models of language

As pointed out by John Hale [17], a current challenge in modern Linguistics is to incorporate it into the general enterprise of Cognitive Science. This means that grammars given by linguistic theory have to incorporate a temporal component to give birth to computational mechanisms, like automaton models, capable of explaining behavior. Nonetheless to bring linguistics into neuroscience we have to go much further and also provide reasonable implementation models conforming to the biological components of the brain. This implementation is necessary to be able to go beyond behavioral measurements and ultimately test computational hypotheses directly against the currently available spatio-temporal neural measurements.

A good example of success in this direction would be the computational theory of visual receptive fields [18] that makes impressively accurate predictions on the shape of the biological visual fields found in the retina. Knowledge of these basic units of visual perception have recently even allowed to correlate the mechanisms behind deep convolutional neural networks to visual pathways [19, 20] and has influenced our understanding of higher-level visual phenomena such as visual illusions [21]. Although expecting at the moment something similar in the case of language might sound overambitious, we must note that basic phonetic features have already been decoded in the Superior Temporal Gyrus from electrocorticography (ECoG) [22], effects of constituency separating syntactic and semantic components across brain areas have been identified with bold-Fmri [4](CP: Hum, maybe a bit exaggerated. Will see if I make a weaker claim.) and recently patterns of the neural temporal dynamics of sentence construction also coming from (ECoG) have been revealed [3, 23]. The recent work from Nelson et al. [3] is particularly relevant to us, since it depicts for the first time a possible neural signature of variable binding, referred by the authors as a'merge' operation, that we will compare qualitatively with our modelling results.

Numerous Artificial Neural Network models for specific and general language tasks have been implemented. For an extensive review of these, categorized by language function, we recommend reading Bocancia [24], Christiansen et al. [25] and Miikkulainen [26]. Among these the Shruti architecture for logical inference [27] and the latest optimization and quantization framework of Smolensky for phonological production [28] are notable mentions. Nonetheless more relevant to our work are efforts to model language function solving the variable binding problem with biological plausible mechanisms. Examples of this are CABot [29], BioPLa [30], TRANNS [24], the language models of Markert et al. [31], the corticostriatal model of Dominey et al. [32], the discrete combinatorial neural assemblies of Pulvermuller [33, 34], the words model of Garagnani et al. [35], the DORA mechanism proposed by Martin et al. for hierarchical linguistic structures [36].

All these efforts have different merits in what they can say about the implementation of language function and have been successful at demonstrating the feasibility of approximating language tasks with biologically constrained neural networks. Nonetheless, even though they attempt to offer biological plausible implementations, many biological details necessary to match in-vivo neural patterns of the modeled processes have been kept out of scope. This has been a reasonable strategy so far considering the computational cost of building circuits with point neural models, but as we will show, recent developments like population density techniques [37] permit to implement state-of-the-art biologically detailed circuits of neural populations. This work has a similar spirit to the Blue Brain Project [38] to tackle the "predictive neuroscience" and "simulating the brain" challenges posed forward by Markram [39]. So instead of trying to implement a complete language parsing neural network trained from stimuli, we will focus on pushing the boundary of biological detail for the specific abstract mechanism of variable binding as proposed in the Neural Blackboard Architecture [1], assuming other necessary mechanisms for parsing are in place. Basically we will implement a simulation that can provide temporally detailed predictions about the neural signature of variable binding, assuming binding by process, and then compare such predictions to actual recordings obtained from ECog and fMRI.

1.2 The Neural Blackboard Architecture (NBA)

The NBA responds to much more than the problem of binding. It addresses all Jackendoff problems [2] and propose a general mechanism applicable to the different stages of language processing that could fulfill the tripartite model of Jackendoff [7]. Its level of abstraction allows its application to any linguistic theory for which a grammar and parsing mechanism is specified and could even be applied to other cognitive functions. At the same time it is sensible to interpret the architecture as a circuit of neural populations, where some of these populations can conceptually be linked to cell assemblies. This is an important assumption of the NBA and there is substantial biological evidence for the existence and functional relevance of cell assemblies as computational units [40]. For example based on the synaptic connectivity patterns of pyramidal neurons in the neocortex, Perin et al. [41] even posed forward the theory of neuronal group selection of Edelman [42] over Hebb's organizational principles [43] that emphasize the role of single neurons in a computational circuit with less connectivity constraints.

There are already several implementations of sub-circuits of the NBA with varying degrees of biological plausibility. Where the latest rely mostly on Wilson Cowan population dynamics [44]. Some of the simulations attempt to address diverse aspects of language processing like ambiguity [45] and learning control from syntactic stimuli [46], while others address circuit related issues like instantiating a connectivity matrix with randomly connected networks [47] and implementing a central pattern generator for

sequential activation [48]. In the following paragraphs we will only summarize the main abstract mechanisms and assumptions behind the NBA. For a deep review we recommend to read recently published circuit design and examples that focus on sentence processing [49] alongside the original framework proposal for combinatorial structures in cognition [1].

The NBA assumes grounded representations of concepts in distributed or local neural population referred to as Main Assemblies (MA). Variable binding of concepts is implemented through the conditional activity of a neural population referred to as Sub Assemblies (SA), driven by MAs. Then SAs lead to the activation of neural populations that portray Delay Activity [50], which can be interpreted as Working Memory (WM). So in the case of sentence processing we can equate the grammatical categories to the grounded concepts of MAs, the parsing process to the conditional activity igniting SAs and the derived syntax tree to the implicit representation given by a collection of WM reverberating populations with delay activity.

To understand how a sentence is processed in a blackboard architecture, we should start by considering the simplest case of binding two grammatical categories. This takes place in one *compartment circuit* of a *connection matrix*. The *compartment circuit* contains the SAs that encode the relationship type of the binding and the WM that keeps the binding for an arbitrary period of time. It is engineered with six simple *gating circuits*. The *gating circuit* can be seen as the smallest meaningful circuit in the NBA, composed of interconnected neural populations such that neural activation is transferred conditionally between a source and target population. Thanks to this, the *compartment circuit* allows bidirectional communication between the MAs encoding the grounded representation of the grammatical categories mediated by a neural control mechanism. Which would permit query operations to take place after the binding has been implicitly encoded with active WM populations, by reactivating the query driven MA and allowing conditional activity to flow towards the answer MA.

Now we are ready to describe the processing of a complete sentence. Basically this takes place in a *blackboard*, which is a set of *connection matrices*. Where each *connection matrix* fixes the memory capacity by determining the possible amount of bindings for a pair of grammatical categories. A *connection matrix* manages memory slots dynamically through competing mutually inhibitory compartment circuits and in this way handles the dynamic binding of a particular pair of grammatical categories. Then all the necessary bindings are determined by the relevant connection matrices available and the number of sentences that can be kept in short term memory are limited by their capacity. Complete illustration of the blackboard architecture is given in Figure 1.

An important feature of the blackboard architecture is its flexibility to process and implicitly represent arbitrary tree structures. Most of the previous blackboard simulations considered flat tree structures corresponding to dependency grammars [51], where as expected the word grammatical categories elicit activity in MAs while their dependencies are represented by activity in WM and SAs. This overlooks other grammar theories that depend on constituency like a phrase structure grammar [52], where it is also necessary to instantiate MAs for phrasal categories. Nonetheless this can be easily resolved by allowing a WM, activated by the binding of two word categories, to instantiate activity in another MA, which can participate in further bindings reflecting hierarchical structure.

Here we implement only the necessary parts of the NBA to model the neural activity related to variable binding, which itself is enough to instantiate the representation of an arbitrary sentence syntactic structure if we take the grammar theory and parsing scheme as given. This means that we simplify two important aspects of the circuit. The first is that we will provide the signals of control directly to the compartment circuits. Previous attempts to train the control mechanism [46] were tailored only to specific

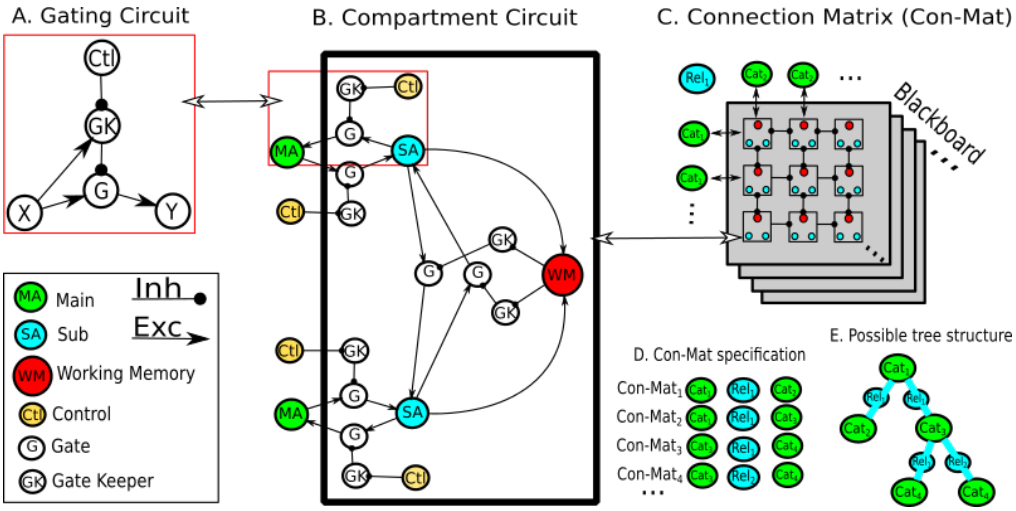

Figure 1. Blackboard architecture. A. Gating circuit that allows the implementation of conditional neural activity transfer between Neural assemblies X and Y through a gate assembly. The gate keeper assembly initially is also activated by the X assembly and then inhibits the gate assembly, so a control assembly has to inhibit the gate keeper assembly to let information flow through the gate assembly. B. Architecture of one compartment circuit of a connection matrix is shown. Six gating circuits are arranged such that conditional bidirectional neural activity flow is possible between two main assemblies. Control assemblies regulate the direction of information flow and allow the activation of sub assemblies. The two sub assemblies excite the working memory assembly which once activated encode the binding of the main assemblies and allow activation to flow between them if the controls allow it too. C. Each connection matrix contain n by m compartment circuits that encode the same relationship type between the same pair of assembly categories. There are m available assemblies for one category and n available assemblies for the complementary category and only one cell circuit can activate its working memory assembly to link two particular assemblies due to mutual row and column inhibition of cells in the connection matrix. The size of the connection matrix effectively represents memory limitations. A blackboard is composed of an arbitrary number of connection matrices that encode different relationship types for a pair of assembly categories. D. A blackboard is composed of multiple connection matrices, where each of them is defined by two node categories and a relationship type between them. E. Example of one possible tree structures out of the infinite that can be represented based on the specified connection matrices.

grammatical cases and creating a general control mechanism to test the neural activity patterns would require a more varied dataset in grammatical categories and would comprise computational linguistic efforts out of the scope of this work. The second is that we do not model the dynamic inhibition of competing blackboard compartment circuits, since this would require hypothesis about the size of the blackboard, which would be related to memory limitations and the total number of possible grammatical categories to link in binary trees, which again would require out of scope computational linguistic efforts. Moreover the simplest selection mechanism behind competing blackboard compartment circuits can be hypothesized to be uniformly random on available compartments. This means that we are only testing the temporal patterns of neural activity linked to a variable binding event in the case of two words association. While in the case of complete sentences we are testing predictions based on the average

neural activity time series of a collection of compartment circuits instantiated as demanded by the given grammar theory and parsing scheme. These time series should allow us to differentiate neural activity from different syntactic tree morphologies and sizes. In this work we will compare the predicted signature of variable binding with ECoG recordings and the predicted average neural time series of complete sentences with Bold-fMRI activation patterns.

2 Methods

2.1 Implementation of the NBA

2.1.1 Simplified approach to the blackboard architecture

The present implementation of the blackboard architecture respects its abstract mechanisms but do not implement them completely. Here we do not simulate complete connection matrices, the compartment circuits mutual inhibition mechanism is an operation for which there is no obvious unique implementation. There is already a proof of concept to understand the implementation of the mechanism in randomly connected networks, nonetheless it does not yet achieve a complete circuit level specification integrated with a complete blackboard architecture [47]. Instead we just instantiate compartment circuits as necessary, since in essence they would be selected randomly in a connection matrix from available compartments in the hypothesized blackboard.

The compartment circuit abstraction is enough to achieve our current simulation goals, since the same mechanism is used in different connection matrices and they might only differ in their memory capacity. So we can consider the same compartment circuit simulation for all different pairs of grammatical categories, where the circuits would have similar dynamics and only vary in activation time of their neural populations. Nonetheless we are only able to ignore the activity of complete connection matrices because we are not planning to explore the effect of memory limits under time compressed sentence processing scenarios or memory tasks. Otherwise important deviations in background neural activity due to depletion of available compartments in the connection matrices and intense inhibitory activity would become a crucial factor in the simulation. This could be an interesting exploration in future work to try to reproduce the temporal bottleneck effects on neural activity shown by Vagharchakian et al. under conditions of compressed speech and reading [53].

In the case of the control mechanism, Feed-forward artificial neural networks have already been employed with the NBA [46] and recently state of the art feedforward network architectures have shown top performance for diverse language parsing tasks [54]. Moreover a more recent extension of the NBA relying on the motor circuit of the marine mollusk Tritonia diomedea to generate patterns for sequential activation control has been proposed [48]. Nonetheless implementing these neural architectures would be out of the scope of this work, since we will not investigate the whole neural activity related to parsing but only the portion specifically related with variable binding, which itself is enough to look into the formation and storage of a phrase structure with temporal events derived from some some given parsing mechanism. Where also the expected phrase structure is given by some specified grammar theory. So we will simply provide the control signals that will allow the necessary neural activity flow from MAs to WM to process the hypothesized syntactic structure as required by a given parsing scheme and grammar theory.

2.1.2 Simulation framework and architectural decisions

Previous simulations of the blackboard approximate the mean activity of neural assemblies with Wilson Cowan dynamics [45]. Nonetheless direct simulations of leaky-integrate-and-fire (LIF) neurons [55] have faster transient behavior than the pseudo dynamics described by the Wilson Cowan equations. Such equations, as explained by De Kamps [56], only allow to approximate correctly the steady state of neural populations by suggesting what mean firing rates should be. On the other hand, population density techniques [57] implemented in the MIIND software [56] [58] can accurately describe the transient dynamics of large populations of the mentioned LIF neurons.

In Figure 2 one can see an important difference between the transient dynamics of the rate-based Wilson Cowan dynamics and the population density techniques. Moreover one can appreciate how well population density techniques approximate the precise simulation of the LIF point neuron model presented by Omurtag [55]. In this work we are interested in modelling the transient dynamics of variable binding with the future aim of comparing the simulation with real temporally detailed patterns of neural measurements like ECoG. So we opted to implement the compartment circuits with population density techniques in MIIND instead of Wilson Cowan dynamics.

One could further argue that it is desirable to implement even more realistic simulations approximating conductance based neural models and neuron point models as those implementable with the RON, GENESIS and NEST software reviewed by Brette et al. [59]. Nonetheless it has been shown that simpler 2D models like adaptive exponential integrate-and-fire (AdEx) can already predict correctly 96% of the spikes of detailed conductance models [60]. Although the model has the strong simplification of only considering one adaptation time constant, when in reality adaption takes palce on multiple time scales, it reproduces many known electrophysiological features, as can be appreciated in the spike-frequency adaptation review of Benda et al. [61, 62]. AdEx can also be approximated with population density techniques and has been recently added to MIIND. Although it is at least two orders of magnitude more computationally expensive than a LIF model, it is feasible to implement it in a circuit with tens of populations like the one we will simulate. So we will implement the circuit under a LIF and an AdEx model to show the effects of adaptation in the neural dynamics of variable binding under the NBA framework. To our knowledge this is the first time that the AdEx model will be employed to approximate the neural dynamics of a circuit of this magnitude reproducing cognitive function.

In the case of Delay Activity (DA) populations like WM, we decided as a first approach to model such mechanism artificially. We plan to address the different alternatives to model persistent cortical activity with interacting neural populations in future work. As suggested by De Kamps [50] not only models of recurrent excitation but also recurrent inhibition can account for this phenomena. In the current simulation a constant firing rate is kicked off by a specified level of input that is sustained for a desired period of time. Contrary to previous simulations [63], we do not consider SAs as DA populations. We find that SAs can show rich and interesting dynamics just by fulfilling their function of mediating activation for WM. In the case of MAs we model them as receiving input from WM populations instead of considering them as another DA population. This is done mostly to separate the notion of a concept stored in a WM from the recruitment of the MAs during parsing that would need to take place during sentence processing. Moreover this allow us to easily instantiate deep tree hierarchical structures by considering the WM of one circuit as the source of activity that drives the MA of the next compartment circuit in the hierarchy. The details of this implementation will become clear in following sections.

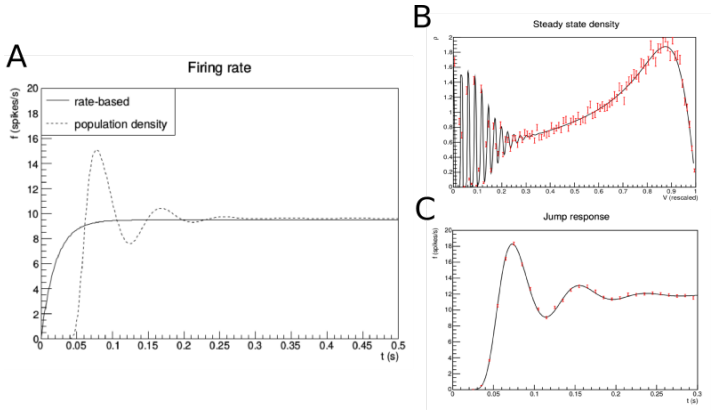

Figure 2. Case for population density techniques over Wilson Cowan dynamics. Plots taken from the MIIND manual. A. Shows the mean firing rate of a neural population simulated with Wilson Cowan dynamics, labeled as a rate based model, and a population density technique with similar mean and standard deviation of neural activity. One can see that the steady state of the population activity converge in time but that the transient dynamics are importantly different. B. Histogram of the membrane potential for each neuron in the population density technique simulation shown in A at time 0.3. The solid line corresponds to the prediction of the population density technique, while the red markers correspond to error bars due to finite sample sizes in a point model simulation performed with NEST. C. The jump response of the neural population according to the NEST simulation and the population density technique. There is complete agreement within the boundaries of statistical error.

2.1.3 Compartment circuit parameters

The compartment circuit contains two different types of neural populations. Artificial neural populations following a boxcar event model and biological neural populations following LIF or AdEx neural models. Both biological neural models have a wide range of parameters that have been tuned in the literature to follow the behavior of a regular spiking pyramidal cell in the cortex according to electro-physiological measurements. These were taken from Omurtag et al. (2000) [55] in the case of LIF neurons and from Brette et al. (2005) [64] in the case of AdEx neurons. As a first step we wanted to only explore the behavior of the circuit of neural populations in generality following well studied sets of parameters. Nonetheless it is clear that studying the neural dynamics of specific brain regions might require adapting the parameters of the neural models to local measurements. Also considering parallely multiple neuron typologies and modelling their corresponding microcircuitry of cortical columns as attempted already with LIF models to simulate local field potentials for a very small patch of cortex [65,66]. Each neural population can be either excitatory or inhibitory and so only connections from the same type can come from them, respecting Dale's law. The biological neural populations are conformed by a pair of Main Assemblies (MA), a pair of Sub Assemblies (SA), six Gate Assemblies (G) and six Gate Keeper Assemblies (GK). On the other hand the artificial neural populations are conformed by Control assemblies (Ctl), Working memory assemblies (WM), Event Input Assemblies (Inp) and a Baseline Assembly (B) that drives baseline neural activity. A complete diagram of the compartment circuit with example parameter values for LIF populations is given in Figure 3.

That the artificial populations follow a boxcar event model means that we just have to specify the starting point of events, the persistent firing rate of the population and the duration of the persistent activity. In the case of the delay activity of WM we also

have to provide a kickoff input rate threshold that automatically triggers the boxcar event instead of providing a start time point. The duration of persistent activity was pragmatically set up long enough to visualize the steady state of the neural dynamics. Finally the persistent activity rate and kickoff rate threshold were arbitrarily selected from feasible parameter range values given by various simulations of the circuit dynamics that will become clear in the following section.

Selecting firing rates to tune the compartment circuit is a complex task given the contrast between the extremely simplified circuit and real neural networks that contain multiple types of neurons with diverging behavior across cortical layers [67]. Wohrer et al [67] shows, from measurements in rat cortex, that the actual firing rate distributions of neural networks do not differ much between resting state and evoked activity. The small difference would come from very few neurons that manage to drive up the mean firing rate in recordings while most neurons in the population are almost silent, some with rates as low as 0.1 Hz [68], whose activity might not even be picked up by most recording devices. Although theoretical analysis of the distribution of firing rates in randomly recurrently connected networks of LIF neurons near the fluctuation-driven regime suggests considering mean firing rates around 6.4 Hz [69]. Based on the review of Wohrer et al. [67], particularly on the firing rate in motor areas of behaving macaques, we decided to kickstart biological neural populations activity up to a conservative baseline firing rate of 1 Hz and study the neural dynamics of circuit input firing rates of up to 10Hz.

There are two parameters governing transmission of neural activity between neural populations. First we consider the synaptic efficacy of connections, which was setup to be homogeneous across the circuit under the lack of appropriate hypothesis to tinker it in a detailed manner. As exposed by London [70], current understanding of synapsis is limited and even contextual measurements of efficacy might be more appropriate to understand the impact of synaptic input on spike output that actual set parameters of the synapse. Moreover recent evidence [71] shows that synaptic efficacy might be modulated by attention processes and is naive to consider it as a fixed parameter in a circuit. The study of Briggs [71] suggest that synchronous firing of neurons with the same input has probabilities between 3.1 and 7.6 while single firing has probabilities ranging from 28% to 36% depending on the type of neurons considered and the attention state. Based on these reports, we decided to verify, through an initial sub-circuit experiment, the effect that synaptic efficacy could have on the circuit temporal dynamics, contrasting a low (10%) and high (30%) value of synaptic efficacy for both LIF and AdEx populations. This allowed us to verify if the tradeoff between efficacy and number of connections was a trivial one, simply requiring more connections when assuming a lower efficacy to attain similar ouput firing rates for the same input rates. This, as will be shown in the results section, was not the case for AdEx populations. Nonetheless the difference in the qualitative nature of the temporal dynamics was confirmed to not be crucial for the circuit setup, so for the remaining simulations we employed the more conservative 10% synaptic efficacy regime.

The second parameter governing transmission of neural activity was the number of connections between a pair of neural populations. Unlike synaptic efficacy, the number of connections were determined from a series of simulation experiments. First the number of connections from baseline persistent activity was set such that, during rest, the circuit steady state activity would stabilize around 1 Hz. The number of baseline connections necessary is a function of input firing rate, synaptic efficacy and neural model, such that a lower synaptic efficacy required a higher number of connections. Then the number of connections coming from excitatory populations was determined such that bidirectional gating circuits would have a stable steady state firing rate when both Gs allow neural activity to be transmited. Finally the number of connections

coming from inhibitory nodes were setup high enough to block neural activity flow in a gating circuit, which means that GKs driven by MAs would be able to completely inhibit activity in Gs. Our simple approach to neural rate transmission ignores many intricacies like activity regimes that might allow rich internal computations. [72]. Also connections distribution might have an impact in spike based communication [73]. Still we decided to keep connections between populations as simple and homogeneous as possible for a first approach.

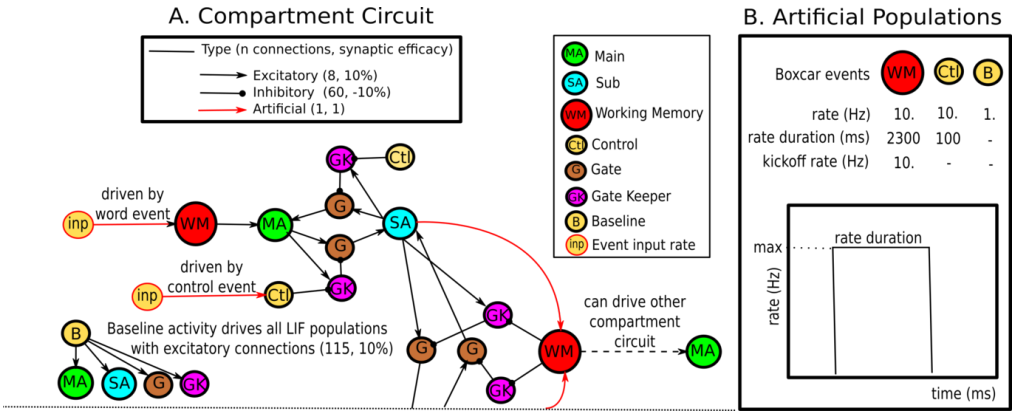

Figure 3. Compartment circuit example A. Details of the Compartment Circuit implementation. Only half of the circuit is shown since the design is symmetric. The baseline (B) and Event input (Inp) populations are part of the simulation and not of the original abstract circuit proposal. B. The behavior of the artificial neural populations and their selected parameters is shown

2.1.4 Simulation experiments performed

Since it is possible to tune the circuit to reproduce arbitrary firing rate values under which circuit dynamics are similar and stable, we simply aimed at picking reasonable parameter values such that the circuit would mantain overall modest firing rate values with respect to the literature of neural measurements. To setup parameters and compare in detail the compartment circuit dynamics for LIF and AdEx neural populations, four simulation experiments were performed taking different sub-circuits into account. A diagram of each sub-circuit is shown in Figure 4. The first simulation simply consists on the activity of one neural population driven by a fix activity rate of 1 Hz. We used this simulation to explore the necessary number of baseline connections to drive baseline activity in the circuit to approximately 1 Hz. The second simulation allowed us to explore how neural activity flows through a chain of neural populations being regulated by a control mechanism. The third simulation explores how neural activity is enhanced by a closed loop between a MA and SA, since it will be the case in the memory sub-circuit that activity is allowed to flow bidirectionally once the WM delay activity is unleashed. Finally the fourth simulation consists on adding GKs to the closed loop sub-circuit of the second simulation to explore how many inhibitory connections are necessary to keep activity from flowing in the circuit unless the controls allow it.

After determining reasonable parameter values, we simulated the complete circuit, portrayed in Figure 3, for both LIF and AdEX neural populations. Then we contrasted the obtained neural patterns of the MA, SA, G and GK neural populations with binding and constituency effects available in the neuroimaging literature. First we show similitudes between the activity of one compartment circuit and ECoG time series

patterns of binding revealed by Nelson et al [3]. We naively compare the firing rates of our simulation directly to the patterns observed in ECoG recordings, considering the correlation that exist between the high gamma power of local field potential signals and firing rates [74, 75]. Nonetheless a quantitative comparison would require a more careful consideration, employing recent models tuned to electro-physiological measurements that offer a way to translate neural activity to local field potentials [65, 66].

Then we simulate the binding activity related to the processing of complete phrases. Assuming a syntactic tree structure given by a phrase grammar theory and the order of control events given by a bottom up parsing scheme. As a first simplified approximation to the NBA dynamics, we instantiated parallely the necessary compartment circuits to represent a complete assumed tree structure. Once we obtained time series for the processing of the entire phrase, by summing activity across similar node categories of the multiple compartment circuits required, we convolved the time series with the Glover Hemodynamic Response Function [76]. This allowed us to approximate the hemodynamic constituency effects depicted by Pallier et al. (2011) [4]. We managed to show that the sublinear function that surprised the authors, governing the amplitude of HRF responses for the different stimuli categories, is approximated by the dynamics of binding events assumed by the NBA.

Since the quantitative level of neural activity can be easily tuned for a wide range of parameter values with similar behavior, when comparing the circuit neural dynamics with the neuroimaging literature, we only focused on the qualitative neural temporal patterns observed. All the C++ scripts behind the circuit and sub-circuit simulations, taking advantage of the MIIND software [56] [58], are accessible in the Blackboard application folder of the MIIND github repository https://github.com/dekamps/miind.

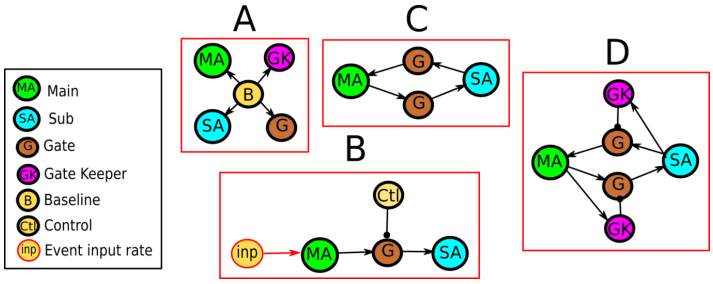

Figure 4. Sub-circuit simulation topologies Each number corresponds to its respective experiment. For better visualization all baseline nodes are excluded from the topologies. A. Single neural population driven by baseline activity. This topology reminds of the fact that all MA, SA, G and GK populations are driven initially in the same way by a persistent baseline fixed rate. B. Chain of populations where activity is temporally interrupted by a control node. C. Closed loop formed by MA, SA and Gs. D. Closed loop broken by the addition of GKs.

3 Results

3.1 Sub-circuit simulations

3.1.1 Experiment 1: Simple neural population

The first experiment allowed us to explore the basic temporal behavior of the different neural models under different synaptic efficacy regimes. It also allowed us to select an appropriate number of baseline connections to tune the steady state firing rate of all

LIF and AdEx neural populations to approximately 1Hz while being driven by a persistent artificial 1Hz baseline rate. As indicated in the topology A of Figure 4, all neural populations are driven identically by a baseline node, so simulating one allow us to get an idea of the behavior of all biological populations in isolation from the circuit connections.

As depicted in Figure 5, the steady state firing rate of LIF populations is a monotonous increasing function of number of connections for both synaptic efficacy values. We can see from the detailed temporal activity that the firing rate increases gracefully until achieving the steady state after approximately 200ms. On the other hand, the AdEx populations behavior is qualitatively affected by the synaptic efficacy value chosen. For a 10% efficacy the steady state behaves like a monotonous increasing function as in the case of LIF populations but for a 30% efficacy we observe a concave behavior due to extreme adaptation that limits the steady state rate to a maximum below 1Hz. If we look at the temporal details, the Adex populations also behave differently from LIF populations. They portray a sudden increase of activity on initial stimulation that is then driven down by adaptation, achieving a steady state after approximately 600ms.

Based on these observations we decided to consider only the low efficacy regime of 10% for the remaining simulations. In the case of LIF populations the higher efficacy would not bring any qualitative modification to the dynamics of the circuit. In the case of the AdEx population the only important qualitative difference would be constraining the use of the steady state rate of activity, which would itself force a tighter coordination of events. This more strict event coordination can also be understood from the more permissive low efficacy regime as will become clear in the following simulations and discussion. Finally we learned that the number of baseline connections that best approximate a 1Hz steady state firing rate are 115 and 1646, for LIF and AdEx populations respectively, which will be fixed for all remaining simulations.

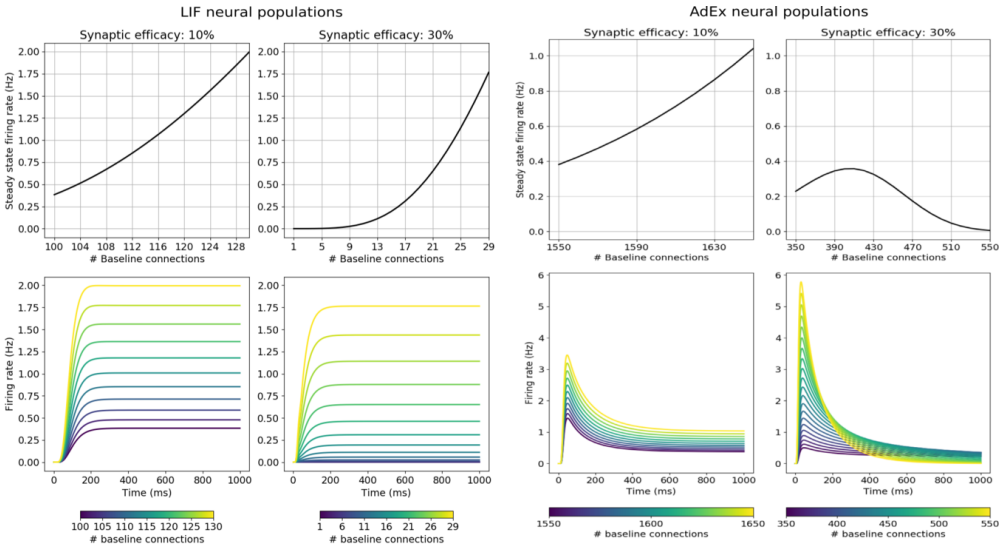

Figure 5. Baseline neural dynamics The plots at the top depict how the steady state rate of a neural population relates to the number of baseline connections under a baseline input of 1Hz. The plots at the bottom show example temporal dynamics corresponding to its upper plot.

3.1.2 Experiment 2: Neural activity flow and control release

In the second experiment we explored how the coordination of input and control events would affect the rate of activity across a chain of neural populations. We employed the topology B of Figure 4, in which a fix input rate drives the activity of the sub-circuit during a given time window and is mediated by a control operating under another time window. This corresponds to a MA that attempts to drive up the activity of G and SA, while a Ctl node inhibits the activity in G and isolates SA activity from the input stimulation. The input and control events can start at any arbitrary moment for any duration and what interests us are the dynamics of the circuit when inhibition, assumed in the complete circuit to be always present, stops allowing MA to freely excite G and SA. There are three extreme cases that characterize the circuit behavior. When the input starts and the circuit achieves the steady state before G inhibition stops (Input first), when G inhibition stops and the circuit achieves a steady state before the input starts (Control first) and when both input starts and inhibition stops at the same moment (Coordinated). Analyzing this sub-circuit let us determine what kind of input rates are necessary to drive the maximum and steady state rate of SA to some desired activation threshold for WM. Moreover it gave insight into what are the most constrained type of events for each neural model.

In Figure 6 we portray the neural dynamics of the last population of the chain (SA). The steady state in a LIF model is achieved at a similar time (under 200 ms) for all event cases. The Input first and Coordinated events have a similar quantitative behavior, which means that the dynamics of stopping inhibition are insensitive to MA having achieved a steady state from the input stimulation. Nonetheless starting the input on the absence of inhibition permits higher initial fluctuations of the firing rate and so higher maximum rates of activity. On the other hand, the AdEx model shows a more complicated behavior. Due to adaptation effects, the maximum output rate response will depend on the current state of the population. Basically the closer the population is to its steady state, the less responsive it will be due to the accumulated adaptation. In AdEx populations the steady state takes longer to be achieved (just approximated after 400ms) and its convergence rate depends on the input rate and events combination. Also the maximum firing rate of the dynamics strongly depends on the event case. Contrary to the LIF model, stopping inhibition in advance minimizes the rate dynamics due to the stronger adaptation present at the steady state of G. Then starting the input before stopping inhibition improves the rate dynamics at G and SA, which increase the further MA is from achieving a steady state after the input starts and so are maximized with perfect coordination of input and control.

From these observations we learn that the combination of events that reduce the most the rate dynamics depend strongly on the neural model selected. Being the Input first or Coordinated cases for the LIF model and the Control first case for the AdEx model. Moreover, as is apparent in Figure 6, the AdEx model requires a higher input rate to achieve modest increases in the steady state of the output rate, which limits the behavior of a circuit of AdEx populations under constant input rates.

3.1.3 Experiment 3: Enhanced neural activity from closed loop

In a third experiment we tested the behavior of the sub-circuit corresponding to topology C of Figure 4. As was mentioned before there is a number of excitatory connections after which the output rate is higher than the input rate, such that populations wired in a closed loop would enter an uncontrolled self reinforced activity regime. Since we expect such a loop to exist in our circuit during activation of WM, we had to constraint the number of excitatory connections employed. Another important implication of the closed loop is that we would expect the steady state activity of the

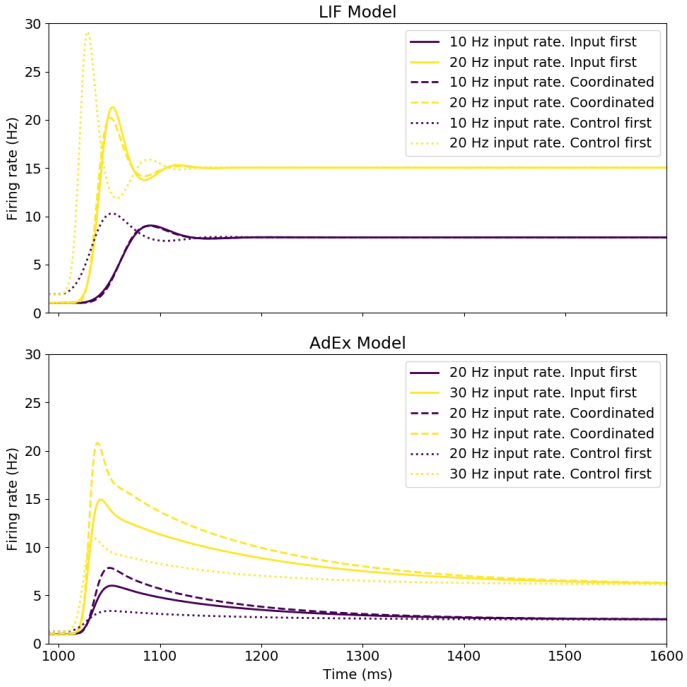

Figure 6. Neural dynamics of input and control events. For each neural model two input rates are simulated with the three extreme combination of events: Input first, Control first and Coordinated. 9 and 20 excitatory connections are assumed for the LIF and AdEx models respectively. We show the time series of the firing rate in the last population of the chain (corresponding to a SA node of topology B in Figure 4).

populations to be higher than in their independent states, which also gives a lower bound to the activation threshold that we can select for WM, since otherwise WM would enter a state of perpetual self activation after being activated the first time. The steady state rate of the closed loop is shown in Figure 7 up to the number of excitatory connections that would lead to an uncontrolled activity regime.

Taking also into consideration the results of the second experiment we can depict valid combinations of input rate, number of excitatory connections and WM activation threshold. In figure 7 we show the steady state rate (SS) curve for the events combination with the lowest rate dynamics and the maximum rate (Max) curve for the events combination with the highest rate dynamics. Notice that, as explained in the previous experiment, the relevant combination of events in the analysis are different in the case of LIF and AdEx populations. These curves delimit four parameter regions with different implications for the behavior of the NBA's memory circuit. The regions refer to the ranges of values that the WM activation threshold can take according to a given input rate and number of excitatory connections. The example curves shown in Figure 7 correspond to an input of 10Hz and 25Hz for LIF and AdEx populations respectively.

The perpetual activation region refers to the area below the steady state of the closed loop activity and is independent of input rate. All other regions depend on the input rate that determines the lowest and highest rate dynamics. The flexible activation region refers to the area between the closed loop curve and the steady state of the event combination with the lowest rate dynamics. An activation threshold in that region would secure activation of WM to any combination of events, which makes it the most desirable range for the activation threshold. The constrained activation region is

bounded by the max temporal rate of the highest rate dynamics and represent the range of values for which the timing of input and control events is constrained. Finally the impossible activation region is above the highest rate dynamics and represent rate values that can not be reached by the circuit dynamics.

Characterizing the activation threshold regions is important to understand the reliability of the circuit when exposed to noisy input rates, arbitrary coordination of events, control mistakes or anticipatory control signals. With precise control of input rates and the timing of events corresponding to bottom up parsing, one could simply select an activation threshold just above the minimum rate dynamics to secure activation from the activity of two SAs. Nonetheless there are other scenarios that we should be able to test with parsing schemes diverging from pure bottom-up parsing, if we interpret prediction as anticipated control activation. In that case, if prediction fails we would be confronted with a control mistake for which we would not want the circuit to perform a binding. This would be illustrated by an input that drives activity in the first MA of a compartment circuit followed by a control event that allows activity to flow from all MAs, while the second MA never receives the input corresponding to the activation of its concept. In such a case one would need the threshold to be higher than the minimum of the impossible activation region for a given input rate and number of excitatory connections, such that the input of one SA alone could not trigger WM. This additional constraint can itself push the activation threshold beyond twice the maximum of the flexible activation region, forcing coordination of at least one input and control event, as can be appreciated for AdEx populations in Figure 7. To allow anticipatory control mistakes for the complete circuit simulation we selected a combination of 10Hz and 20Hz input rates, 8 and 20 excitatory connections and 10Hz and 9Hz activation thresholds for LIF and AdEx populations respectively.

3.1.4 Experiment 4: Inhibition of closed loop enhanced neural activity

For the fourth and last sub-circuit experiment, corresponding to topology D of Figure 4. We aimed at tuning the amount of inhibitory connections in the circuit such that the neural activity in GKs could inhibit the activity in Gs when there is no intervention of control signals. In this way we break permanently the closed loop of activity unless a bidirectional control signal or WM activation allows it in the complete circuit dynamics. To realize this we picked the number of inhibitory connections necessary to inhibit max firing rates for the wide range of number of excitatory connections allowed by the closed loop dynamics. The maximum firing rate is employed instead of the steady state rate to observe inhibition of the strongest fluctuations. Based on the curves shown in Figure 8, we set the number of inhibitory connections to 70 and 250 for LIF and ADEX populations respectively for the following simulations.

3.2 Complete compartment circuit simulations

After selecting a valid set of parameters from the observations of the sub-circuit experiments we explored the behavior of the complete compartment circuit simulation. The dynamics of the compartment circuit can be summarized by a combination of the input events that drive activity in MAs and the control events that inhibit GKs such that activity can flow from MAs to Gs and SAs. In Table 1 we present a summary of the parameters for LIF and AdEx simulations and in Figure 9 we present the temporal dynamics of the compartment circuit under different combination of events.

First we observed the dynamics of the circuit when no events take place, leading to baseline activity. In this state all biological populations are just receiving an input baseline rate of 1 Hz from the artificial baseline neural population. Nonetheless instead of having an output rate approximating 1 Hz as they would have in isolation, the

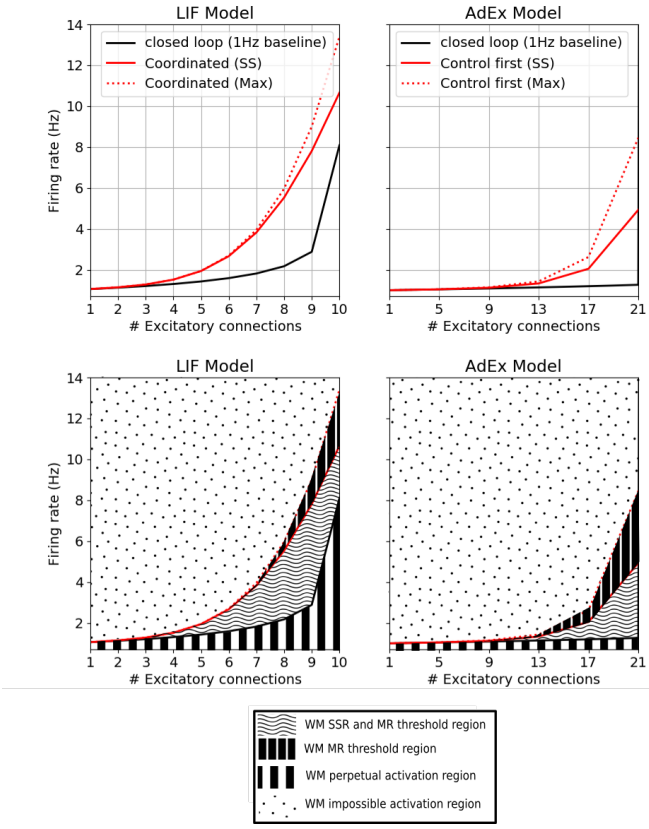

Figure 7. Closed loop activity and memory sub-circuit activation regions. Plots at the top show an example steady state and max activity rate of the event combination with weaker rate dynamics, in contrast to the steady state rate of the closed loop enhanced activity formed by WM activation. Plots at the bottom identify the parameter regions, where the WM steady state rate (SSR) and maximum rate (MR) threshold region is the one that gives most constrained range of circuit parameters to offer the most flexible coordination of input and control events. The event rate curves correspond to an input rate of 10Hz and 25Hz for the LIF and AdEx models respectively.

Parameter	LIF	AdEx
baseline connections	115	1646
excitatory connections	8	20
inhibitory connections	70	250
Baseline rate (Hz)	10	20
WM/Ctl rate (Hz)	10	20

Table 1. Complete simulation parameters

different nodes reflect with their firing rate the architecture of the circuit. Gs show a low rate of activation due to GKs inhibition, while GKs how the highest rate driven by MA and baseline activity. MAs show an activation close to the approximated 1Hz baseline as well as SAs that have been isolated in the circuit thanks to GKs inhibition. SAs have a slightly higher steady state rate than MAs since they are the center recipient of neural activity of the circuit and at least some neural activation manages to leak the Gs. The baseline activity of the different neural models can be seen in part A of figure 9.

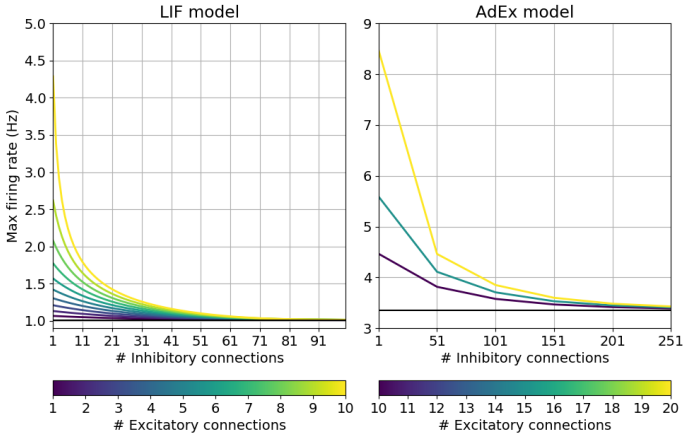

Figure 8. Inhibition of closed loop neural activity Each curve represents how the maximum enhanced neural activity of a closed loop circuit with a given number of excitatory connections is driven back to baseline as we increase the number of inhibitory connections. Considering a baseline rate approximating a 1 Hz steady state in both Models. The maximum firing rate is employed instead of the steady state rate to observe inhibition of the strongest fluctuations.

Then in part B of Figure 9 we portray the partial activity of the circuit. This means that only one MA receives a fix input rate and a Ctl event takes place opening activity flow from both MAs to SAs. We can observe that, as expected, the increased activity of the stimulated MA causes strong inhibitory activity in the GK that compensate the flow of neural activity from MA to G to avoid activation of the corresponding SA. Moreover it can be seen in Figure 9 that in the case that Ctl activation takes place when only one MA is active, the circuit effectively do not activate the binding WM and will simply return to an appropriate steady state once Ctl stops.

Finally in part C of Figure 9 we can appreciate that in case both MAs are active and a Ctl event takes place, then the binding will take place by activation of WM. During the process of binding the reverberating activity of WM that inhibits the GKs connecting SAs creates a sudden burst of activity leading to a pronounced spike as SAs become part of a self excitatory closed loop, also elevating the activity of Gs and GKs between them. This burst of activity quickly drops back to a steady state that leaves the inner circuit in a higher level of activity with respect to its original resting state, facilitating communication between MAs. A similar behavior during sentence parsing was observed in previous simulations of the NBA [45].

Although the general qualitative behavior of the compartment circuit architecture is similar for LIF and AdEx populations, there are three important quantitative differences present but not easy to appreciate in Figure 9. The first is that LIF population dynamics take longer to transmit rates of activity since its transient oscillations are more modest in proportion to the input rate. In these simulations, with the same timing of events, WM became active 86 ms after all input and control events take place in the LIF simulation, while in the AdEx simulation this only took 42ms. The second is that the new enhanced activity regime produced by WM activation is very sensitive to the adaptation effect present in the AdEx model. Not only the parameters of the neural model itself but also synaptic efficacy could completely eliminate the higher sustained activity while keeping a high spike of activity on the moment that binding takes place.

The third is that the AdEx simulation is sensitive also to small variations in the timing of events due to the increasing influence of adaptation as populations reach the steady state, while LIF model dynamics are only affected by the input rate of the events.

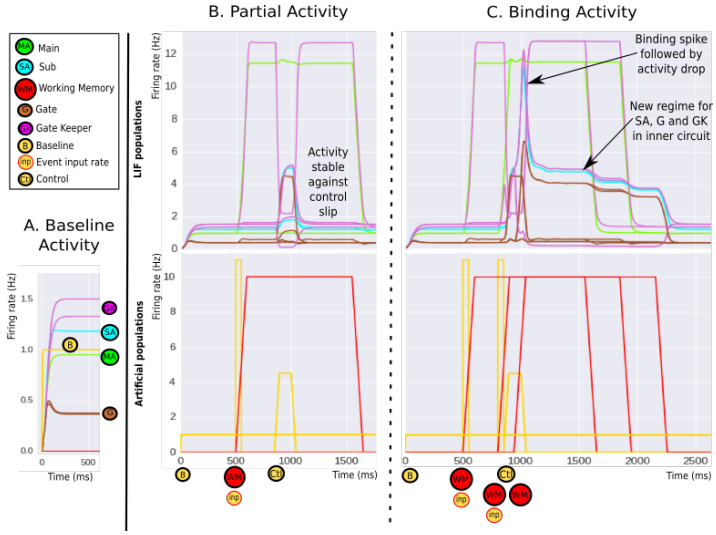

Figure 9. Profiles of neural activity A. Neural activation driven only by baseline input. B. Neural activation of the circuit when only one MA is activated by a word event or WM at 500ms. Portrays the neural activity related to an erroneous control signal at 850ms. Its possible to see that the steady state of neural activity is resilient to a slip of control, going to the appropriate levels of neural activity once the control activity is over. C. Neural activity of the Compartment Circuit for a successful binding. The second MA gets activated at 800ms followed by the controls at 850ms. Since both MAs are active, the SAs manage to activate WM to instantiate the binding of the MAs. Two interesting dynamics arise from the binding. The first is that a spike of activity in SAs, GKs and Gs takes place due to the sudden inhibitory activity of WM on the GKs. The second is that the circuit internally raises its baseline activity.

Once we have the neural dynamic of the compartment circuit, we can extract key segments of transient activity and approximate the NBA binding activity of complete phrases. For this approximation we can consider parallely the necessary compartment circuits to build an assumed underlying tree data structure given by a grammar theory. We would also need a specification of the timing of parsing operations and the desired duration of WM activity. The order of the parsing operations can be taken from a bottom-up or more generalized left-corner parsing scheme. Then the more precise timing of the parsing operations can be assumed to depend on word presentation times for word bindings and minimal operational constraints. Furthermore, we can think of the WM of word bindings as the MAs of phrasal nodes and so on, which would then give us the time at which a superior phrasal nodes input is available.

One can see in the example of Figure 10 how the hypothesized tree structure of a sentence and the timing of the activation of tree nodes is transformed into the neural activity of a blackboard. First we substract the baseline activity profile from the binding activity profile of the segments of neural dynamics used for the simulation. This is motivated by our interest in making comparisons with neuroimaging data. Then we simply add up the aligned time series of the different compartment circuits by neural population category or some other desired criteria. In the example, summaries of the activity of different neural populations are shown as well as total activity of the

blackboard circuit assuming equal contribution from the different populations. Certainly the way we should aggregate time series to compare them quantitatively with neuroimaging data would depend on the spatial and temporal resolution available and the assumptions made about the spatial distribution of the blackboard architecture in the cortex. in the case of WM activation it is reasonable to assume a duration at least long enough to allow all bindings in the tree to take place at the rate that words are presented to the blackboard. In this example words are presented every 600 ms, so for illustrative purposes we assume WM is active 2300ms to be able to bind the first word to an awaited phrase node activated after presentation of the fourth word. If WM was active for say less than 1900ms then activation of the first word MA would cease before the accompanying phrasal node MA comes into play.

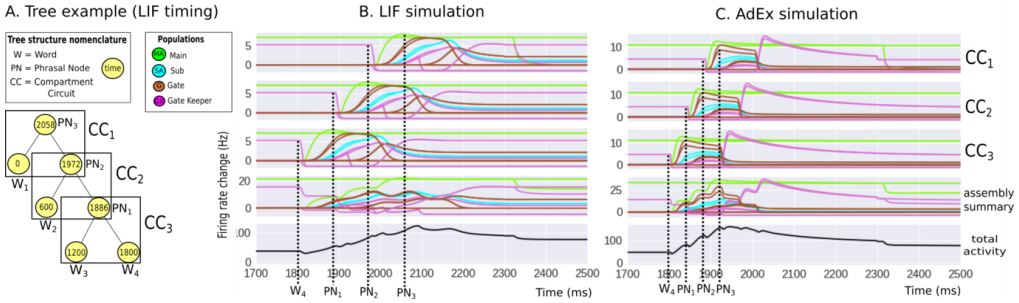

Figure 10. Sentence processing example A. Tree structure hypothesized for a given 4 words phrase. It is shown how compartment circuits correspond to sections of the tree structure and how the nodes corresponding to grammatical categories of words processed or phrase nodes are instantiated in time under a bottom-up parsing approach. B. Blackboard time series that correspond to the simulated processing of the considered tree structure and time of activation of the nodes. The separate activity of the LIF populations of each compartment circuit are shown separately, followed by their summary and total activity C. Same as B but for AdEx populations.

We can apply the complete phrase neural time series approximation to a variety of stimuli from experimental designs behind neuroimaging results in the literature. First we considered the simple case of increasing size right branching trees that relate to a recent analysis of intracortical (ECoG) recordings of a phrase reading task [3]. In this experimental design subjects had to keep a phrase in memory to later compare it with a shorter probe phrase. We make a qualitative comparison with caution, given that high gamma power has been shown to be correlated to the firing rate time series of spiking neurons from in-vivo recordings [74]. In our simulation, shown in Figure 11.A, we can appreciate four main temporal segments of neural activity. An initial increase of activity dependent on word presentation that reflects MA populations, a sudden rise and drop of activity during WM activation, a decrease of activity paced by the duration of input activity driving MA populations and a final drop of activity when WM delay activity stops and the inner closed loop of populations in the memory sub-circuit go back to its initial baseline state. We also show, in Figure 11.B and 11.C., modified plots, extracted from Nelson et al., reflecting the mean high gamma power time series of the ECoG recordings.

As can be seen in Figure 11.B, there is an increase in baseline activity when comparing the beginning and end of phrase processing that can be interpreted as WM related activity based on the task. This memory effect is reproduced in the NBA simulation by the enhanced activity of the closed loop in the memory sub-circuit. It is represented by the difference between the start of the simulation and the end of the MA

inactivation temporal segment, denoted in Figure 11 by black bars. It could further be tuned to fit quantitatively the data by manipulating the number of excitatory connections, such that their decrease would reduce the baseline difference. The irregularities of the magnitude of the baseline effect with respect to phrase length in the high gamma power is difficult to interpret, since it could suggest that the accumulation of activity with more recruiting nodes is subtler than what we can reproduce with the NBA circuit, in which there is a clear correspondence with the number of hypothesized compartment circuits of the parsed tree structure. Moreover, when comparing simulations, we appreciate that the AdEx model could better reflect a more modest proportional increase of baseline thanks to adaptation.

Another observation of the experiment is a proportionally important increase in activity during word processing. The peak magnitude and onset of this increase seems to reflect the length of the phrase. This effect can be captured by the simulation with a simple interpretation of the accumulation of MA activity waiting to participate in bindings, assuming a bottom-up parsing scheme. Nonetheless what was unexpected is the spike of activity followed by a pronounced drop suggested naturally by the NBA simulation, which is also emphasized by Nelson et al. in Figure 11.C. This seems to be the case for both intermediate and final bindings, with a drop magnitude dependent on the number of open nodes in the assumed phrase grammar tree structure of the phrases. The number of open nodes reflect accumulation of pending bindings under a bottom-up parsing scheme in right branching sub-trees. The increasing drop magnitude is captured in the simulation by the quick succession of pending bindings in a tree structure. In the case of the LIF simulation, there is flexibility to extend the activity peak with the duration of control events and to increase the total drop magnitude by manipulating the input rates and excitatory connections. On the other hand the AdEx model loses this flexibility due to adaptation but better emphasizes the contrast between the activity peak and sudden drop because of the pronounced initial activity burst of its population dynamics.

There is an issue with the interpretation of activity drops due to binding operations. As can be seen in Figure 11.B, for the assumed right branching phrase “ten sad students of Bill Gates”, there is a sentence middle drop that do not correspond to the prediction of a completely bottom up parsing scheme. To accommodate this behavior into the NBA, without changing our grammar and parsing assumptions, we would need to incorporate a limited capacity to sustain MA activity that has to be renovated or a greedy binding mechanism that leads to premature binding mistakes. In the case of the sentence end, the final activity drop has a steeper slope than the activity raise during sentence processing, suggesting to incorporate a mechanism that releases MA activity after binding takes place, which is unaccounted for in the simulation. Finally in the analysis of Nelson et al. there is no depiction of WM inactivation, likely due to the experimental design. Interestingly, the AdEx simulation distinguishes itself from the LIF simulation, during WM inactivation, by predicting a final burst of activity due to the inhibition release of the GKs in the memory circuit. Nonetheless this would be a difficult to appreciate marker in the oscillatory signal of intracortical recordings.

We also considered the case of a more complex experimental design employed to show constituency effects with Bold-fMRI [4], also based on right branching trees. In this experiment each stimuli presented to a subject in a trial consisted of a list of phrases with the same number of words (constituents), such that in total 12 words would be presented. The conditions were one list of 12 unconnected words (c01), 6 phrases of 2 words (c02), 4 phrases of 3 words (c03), 3 phrases of 4 words (c04), 2 phrases of 6 words (c06) and 1 phrase of 12 words (c12). This stimuli was simulated by repeating and adding the time series of each of the right branching trees in a condition. In figure 12 we contrast the NBA neural activity time series predicted by the LIF and

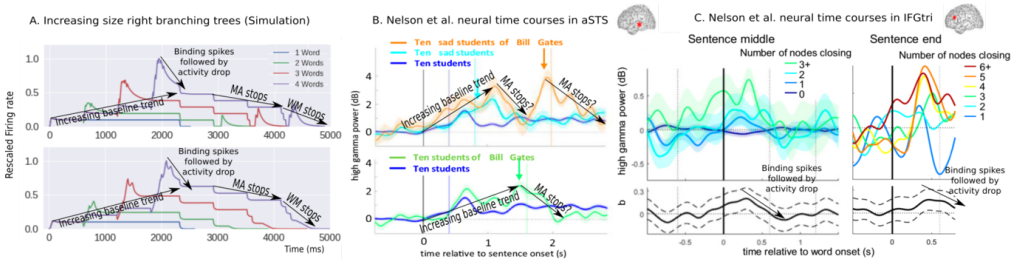

Figure 11. Simulation comparison with intracortical (EcoG) recordings

AdEx simulations for each condition with the simple Boxcar event model used in experiments to estimate the amplitude of the hemodynamic responses. We applied with a convolution operation, to each time series, the Hemodynamic Response Function (HRF) proposed by Glover [76], taken from the python open source package Nistats (**MISSING REFERENCE**). This is a very naive approximation taken for illustrative purposes, that has to be interpreted with caution since the relationship between neural activity, cerebral blood flow and blood oxygenation is not linear [77, 78] and better represented by the balloon model than the gamma function considered here [79].

In Figure 12 we mark the HRF peak and its onset with black lines on the HRF convolved time series. It can be appreciated that the neural time series would predict in all cases a peak onset displaced many seconds with respect to the traditional boxcar event that only represents the duration of the stimuli. Looking at the time series this would be expected, since the HRF peak onset depends on the center of mass of the accumulated response that continues several seconds after stimuli presentation. Nonetheless a precise onset estimation depends on the MA and WM inactivation periods that have been arbitrarily set in the simulation to a constant, which leads to a superlinear increase of onset based on number of constituents. This is unlikely from our previous observations in ECoG recordings, that suggest a much faster decrease of activity after stimuli presentation. Still this prediction gives a cautionary tale on the extent to which lack of neural modelling can lead to a non trivial misspecification of the events introduced in the GLM model to analyze Bold-fMRI experiments. Thinking the other way around, the peak onset link to the MA and WM inactivation periods suggest that we could also use Bold-fMRI to fit the parameters of an inactivation mechanism in the NBA. To realize this, such mechanism would need to be proposed and a more realistic mapping from neural activity to blood oxygenation would need to be implemented. As a last remark related to HRF peak onset, one can appreciate that the LIF neural model introduces an additional onset delay with respect to the AdEx neural model, due to its slower activation of bindings.

On the other hand, both AdEx and LIF simulations predict a similar pattern on the increase of the amplitude of the HRF peak for conditions with increasing constituent size. Since the peak depends mostly on the number of nodes of the assumed tree structures, it is more interesting to compare it qualitatively with the experiment. Our simulations reproduce the sub-linear response that surprised initially the authors, who were testing a linear hypothesis. In addition to normal phrases, Pallier et al. designed a jabberwocky stimuli in which function words are preserved and other words are replaced by morphological similar but undefined words. While there are constituent responses in the language areas TP, aSTS, pSTS, TPJ, IForb and IFtri, only the regions pSTS, IFGorb and IFGtri portray a similar response pattern even when minimizing the semantic content of phrases with jabberwocky. Since our simulation puts aside semantic considerations, this type of experimental manipulation is a better reflection of the activity linked to the compartment circuit of the NBA, in contrast to the aSTS time

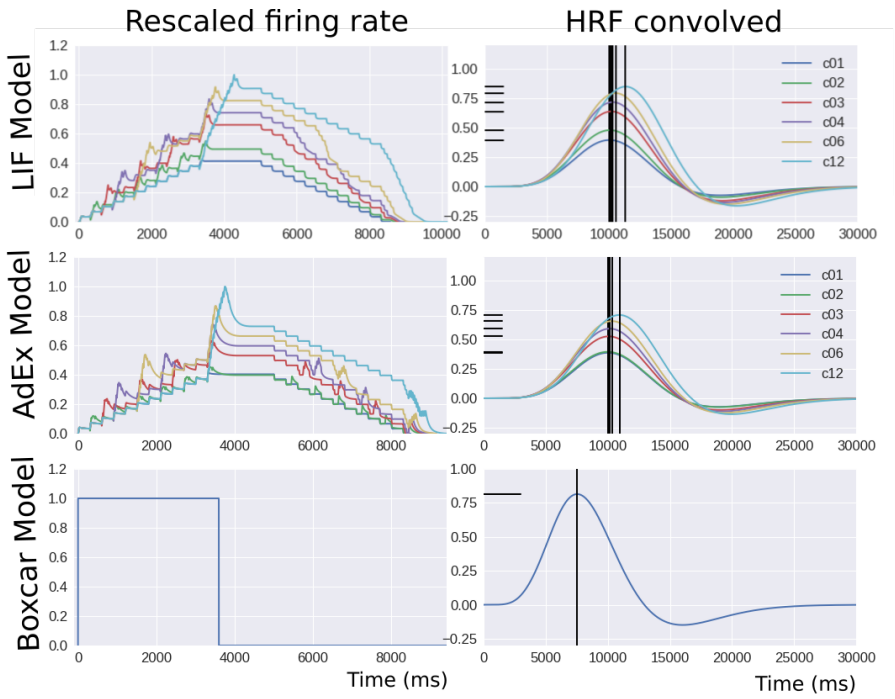

Figure 12. Simulation hemodynamics interpretation

series previously analyzed on the ECoG dataset.

We portray in Figure 13 the simulations predicted pattern alongside the ones revealed in pSTS, IFGorb and IFGtri language regions for the jabberwocky stimuli. The LIF and ADEX predictions are very similar, except for the word list condition. Notice that the contrast of the amplitude of word lists with the other conditions can give insights into the relative proportion between MA and WM activity. As we saw in the ECoG time series, MA seems to have a more important participation in the total neural activity than we initially modeled. This could explain the flatter slope of the experimental results. To reproduce it with our simulations, keeping their qualitative behavior intact, we could select a parameter regime with less excitatory connections and higher input rate. Note that in the case of the AdEx model, due to the shape of the adaptive response, it would be possible to reproduce the sublinear peak amplitude effect while minimizing a peak onset difference. To achieve this we could make all responses approximate the same center of mass by mixing the high initial increase of firing rate, that depend mostly on the input rate, with a very low steady state rate. Nonetheless, to make a quantitative fit to the hemodynamic amplitudes we should use a more realistic hemodynamic model and be cautious about the possible model misspecifications introduced by the simultaneous consideration of the HRF peak onsets.

4 Discussion

An important insight from this work is the sensitivity of the neural activity interpretation to the underlying neural model selected. Even in the case of hemodynamic responses that average out circuit details, we find trade-offs between the LIF and AdEx models. For example that an AdEx model would offer more flexibility in our circuit to manipulate HRF peak amplitudes while minimizing their onsets. To our knowledge this is the first work to explore more complex models like AdEx alongside

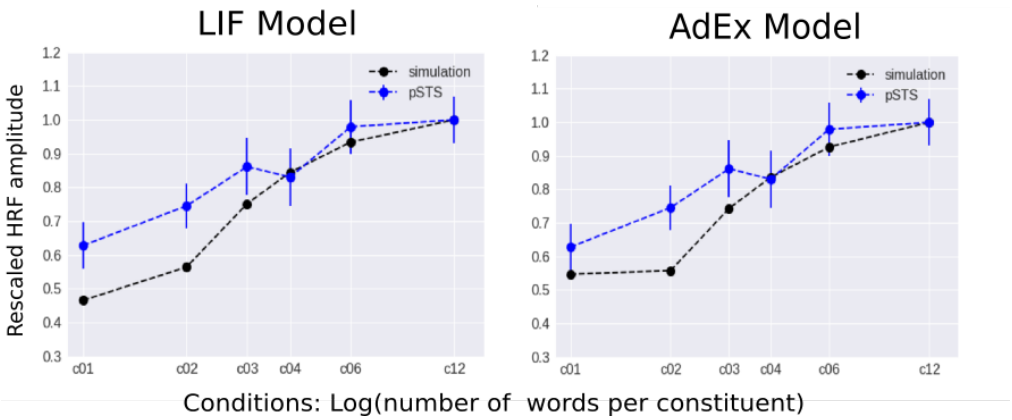

Figure 13. Simulation comparison with Bold-fMRI experiment

LIF for variable binding and language function related circuits. There were also many predictions of the NBA independent of the model selected, like the fact that we need a high number of inhibitory connections and so of inhibitory activity to avoid uncontrolled regimes of self excitatory activity dependent on the connectivity of the circuit.

A more subtle exploration that was considered out of the scope of the work would be to appropriately consider the cell parameters in the models based on electrophysiological recordings from specific brain regions, in contrast to the Omurtag [55] Brette et al. parameters [64]. There are indeed different adaptation constants along the cortex and we have compared the simulation constantly with specific language related brain regions like aSTS, pSTS, IFGtri and IFGorb.

In the case of the complete circuit assumptions, some of them were still overly simplistic. We approximate baseline dynamics with a simple low constant input rate instead of also considering the natural oscillatory activity of the cortex, more appropriate homeostatic mechanisms in cortical circuits [80] and balanced networks [81]. Setting up the synaptic distribution of the network have important implications in terms of energy consumption, while allowing random connectivity could importantly constrain control of closed loop connections. This last consideration is interesting in itself as a research question and could have an impact in the study of the temporal bottlenecks observed in language processing [53]. Introducing modular cytoarchitectonic considerations on the populations that conform the circuit would allow a better spatial interpretation of the circuit activity in a cortex patch and might be anyway necessary to accurately translate firing rates into Local Field Potentials [65,66], hemodynamics [78] and other promising measurement techniques.

Moreover the nature of WM delay activity was left out of the current work due to its flexible and still debated implementation [50], but studying it could reveal important neurobiological limitations on the way we asses the proportion of MA and WM activity and the spatio-temporal memory limitations of the circuit. A final missing consideration that has been partially tackled in previous work [47] is how such a circuit architecture can be formed during learning and brain development. We obviously do not expect the hardwired architecture modeled here to represent the biological reality but to facilitate an approximation to its behavior. Demonstrating how mechanisms approximated by the architecture can actually be learned with biological realistic Hebbian or STDP rules alongside random connectivity constraints, during development, is an important avenue of future research.

The simulation results show how both the steady state and transient dynamics of the circuit affect our interpretation of the neuroimaging evidence for language

processing. In contrast to previous simulations [45–48], employing population density techniques implemented in the MIIND software [56, 58] allowed us to approximate well transient temporal dynamics. Thanks to this, we could show an important difference in the shape of the AdEx and LIF responses, how before arriving to a steady state AdEx responds differently to additional input due to adaptation and how the coordination of input and control events is importantly influenced by the model and its parameters. This last point is crucial for language processing, since ideally we would want input and control events to be as independent as possible to diminish operational complexity and to be able to operate under a wide range of parameters allowing for random variation. Reflecting on the coordinating complications introduced by adaptation we would expect lower adaptation in language related brain regions that seem to be involved in binding operations like pSTS, IFGTri and IFGorb, an increase in the operational complexity of the circuits and/or a reduction in the operational parameter ranges alongside additional sensitivity to noise. A final remark related to event coordination problems in AdEx would be its sensitivity to the synaptic efficacy parameter of the circuit that was not explored in detail. Contrary to the LIF model, AdEx requires clear limitations in the populations connectivity to implement arbitrary or complex timing operations.

An important aspect of this work, that could be overlooked, is the flexibility of the simulation to represent the neural activity of many grammar theories and parsing schemes. We can without circuit modification implement any concept represented as a binary tree. This corresponds well for example to the phrase grammar of the minimalist program of Chomsky [82] and to grammatical relations in dependency grammars [51]. Nonetheless in the case of dependency grammars we would not need to extend the memory of MA less than in a phrase grammar that requires to wait for the instantiation of phrase nodes in deep hierarchical trees. Also the AdEx model would favor shallower tree representations, because it is sensitive to complex event coordination.

Also so far we have implicitly considered activation of phrase nodes only as a result of word binding, which would be representative of a bottom-up parsing approach. This allowed us to simply take the binding WM activity of one compartment circuit as the MA of another compartment circuit. Nonetheless we did not introduce additional delays in control, since we did not model the portion of the NBA responsible for control. Naturally there are many additional parsing mechanisms that we could assume, represented by the order of input and control events, that would introduce predictive control activity. This would be the case if we extend our analysis to the generalized left corner parsing proposed by Hale [17]. We could interpret this additional predictive control signals as control anticipation or as direct activation of memory circuits that have to be deactivated later by an error signal. Exploring the neural activity implications of both these mechanisms alongside the target tree structures given by alternative grammar theories is an important target of future research. This could be done for example by using the simulation as an experiment design tool that provides the set of phrases that maximize the spatio-temporal differences in neural responses across conditions defined under the different grammar theories and parsing schemes.

Finally, even though there are still many limitations in these simulations, we would like to emphasize the quick progress in the development of biologically plausible models of cognition. With an additional effort it would be possible to fit parameters of the circuit and phrase processing directly to neuroimaging measurements. Also diverse new computational methods like population density techniques have made it feasible to approximate at a circuit scale point neural models as complex as the adaptive exponential. There are as well successful recent efforts in modeling, with cytoarchitectonic details, complex signals like Local Field Potentials [65, 66] and hemodynamics with the balloon model [78]. These could be already adapted to our circuit simulations to better incorporate neuroimaging evidence simultaneously from

multiple techniques and experimental designs. Moreover the circuit itself can become a tool for hypothesis exploration and experimental design on the different neuroimaging techniques. In conclusion we hope to have shown that we are close to producing biologically realistic mechanistic neural models of cognitive function, that could provide new ways of testing cognitive hypothesis on varied neuroimaging techniques, to further inspire more work in this direction.

References

1. van der Velde F, de Kamps M. Neural blackboard architectures of combinatorial structures in cognition. Behavioral and Brain Sciences. 2006;29(01).
2. Jackendoff R. Combinatoriality. In: Foundations of Language. Oxford University Press; 2002. p. 38–67. Available from: https://doi.org/10.1093%2Facprof%3Aoso%2F9780198270126.003.0003.
3. Nelson MJ, Karoui IE, Giber K, Yang X, Cohen L, Koopman H, et al. Neurophysiological dynamics of phrase-structure building during sentence processing. Proceedings of the National Academy of Sciences. 2017;114(18):E3669–E3678. doi:10.1073/pnas.1701590114.
4. Pallier C, Devauchelle AD, Dehaene S. Cortical representation of the constituent structure of sentences. Proceedings of the National Academy of Sciences. 2011;108(6):2522–2527. doi:10.1073/pnas.1018711108.
5. Dehaene S, Meyniel F, Wacongne C, Wang L, Pallier C. The Neural Representation of Sequences: From Transition Probabilities to Algebraic Patterns and Linguistic Trees. Neuron. 2015;88(1):2–19. doi:10.1016/j.neuron.2015.09.019.
6. Chomsky N. Problems of projection. Lingua. 2013;130:33–49. doi:10.1016/j.lingua.2012.12.003.
7. Jackendoff R. The Parallel Architecture. In: Foundations of Language. Oxford University Press; 2002. p. 107–151. Available from: https://doi.org/10.1093%2Facprof%3Aoso%2F9780198270126.003.0005.
8. Marcus G. The Algebraic Mind: Integrating Connectionism and Cognitive Science. MIT Press; 2001.
9. von der Malsburg C. The Correlation Theory of Brain Function. In: Models of Neural Networks. Springer New York; 1994. p. 95–119. Available from: https://doi.org/10.1007%2F978-1-4612-4320-5_2.
10. von der Malsburg C. The What and Why of Binding. Neuron. 1999;24(1):95–104. doi:10.1016/s0896-6273(00)80825-9.
11. Feldman J. The neural binding problem(s). Cognitive Neurodynamics. 2012;7(1):1–11. doi:10.1007/s11571-012-9219-8.
12. Smolensky P, Legendre G. The harmonic mind: From neural computation to optimality-theoretic grammar (Cognitive architecture), Vol. 1. MIT Press; 2006.
13. Shastri L, Ajjanagadde V. From simple associations to systematic reasoning: A connectionist representation of rules variables and dynamic bindings using temporal synchrony. Behavioral and Brain Sciences. 1993;16(03):417. doi:10.1017/s0140525x00030910.

14. Plate TA. Holographic reduced representations. IEEE Transactions on Neural Networks. 1995;6(3):623–641. doi:10.1109/72.377968.

15. Chalmers DJ. Syntactic Transformations on Distributed Representations. In: Connectionist Natural Language Processing. Springer Netherlands; 1992. p. 46–55. Available from: https://doi.org/10.1007%2F978-94-011-2624-3_3.

16. van der Velde F, de Kamps M. The necessity of connection structures in neural models of variable binding. Cognitive Neurodynamics. 2015;9(4):359–370. doi:10.1007/s11571-015-9331-7.

17. Hale JT. Automaton theories of human sentence comprehension. CSLI Publications; 2014.

18. Lindeberg T. Normative theory of visual receptive fields. arXiv preprint arXiv:170106333. 2017;.

19. Guclu U, van Gerven MAJ. Deep Neural Networks Reveal a Gradient in the Complexity of Neural Representations across the Ventral Stream. Journal of Neuroscience. 2015;35(27):10005–10014. doi:10.1523/jneurosci.5023-14.2015.

20. Eickenberg M, Gramfort A, Varoquaux G, Thirion B. Seeing it all: Convolutional network layers map the function of the human visual system. NeuroImage. 2017;152:184–194. doi:10.1016/j.neuroimage.2016.10.001.

21. Eagleman DM. TIMELINE: Visual illusions and neurobiology. Nature Reviews Neuroscience. 2001;2(12):920–926. doi:10.1038/35104092.

22. Mesgarani N, Cheung C, Johnson K, Chang EF. Phonetic Feature Encoding in Human Superior Temporal Gyrus. Science. 2014;343(6174):1006–1010. doi:10.1126/science.1245994.

23. Fedorenko E, Scott TL, Brunner P, Coon WG, Pritchett B, Schalk G, et al. Neural correlate of the construction of sentence meaning. Proceedings of the National Academy of Sciences. 2016;113(41):E6256–E6262. doi:10.1073/pnas.1612132113.

24. Bocancia I. A psycholinguistically motivated neural model of sentence comprehension. Universität Ulm; 2014.

25. Christiansen MH, Chater N. Connectionist Natural Language Processing: The State of the Art. Cognitive Science. 1999;23(4):417–437.

26. Miikkulainen R. Natural language processing with subsymbolic neural networks. Neural network perspectives on cognition and adaptive robotics. 1997; p. 120–139.

27. Wendelken C, Shastri L. Multiple instantiation and rule mediation in SHRUTI. Connection Science. 2004;16(3):211–217. doi:10.1080/09540090412331311932.

28. Smolensky P, Goldrick M, Mathis D. Optimization and Quantization in Gradient Symbol Systems: A Framework for Integrating the Continuous and the Discrete in Cognition. Cognitive Science. 2013;38(6):1102–1138. doi:10.1111/cogs.12047.

29. Huyck CR. A psycholinguistic model of natural language parsing implemented in simulated neurons. Cognitive Neurodynamics. 2009;3(4):317–330. doi:10.1007/s11571-009-9080-6.

30. Rosa JLG, da Silva AB. Thematic role assignment through a biologically plausible symbolic-connectionist hybrid system. In: 2004 IEEE International Joint Conference on Neural Networks (IEEE Cat. No.04CH37541). IEEE;.Available from: https://doi.org/10.1109%2Fijcnn.2004.1380167.

31. Markert H, Knoblauch A, Palm G. Modelling of syntactical processing in the cortex. Biosystems. 2007;89(1-3):300–315. doi:10.1016/j.biosystems.2006.04.027.

32. Dominey PF, Inui T, Hoen M. Neural network processing of natural language: II. Towards a unified model of corticostriatal function in learning sentence comprehension and non-linguistic sequencing. Brain and Language. 2009;109(2-3):80–92. doi:10.1016/j.bandl.2008.08.002.

33. Pulvermüller F, Knoblauch A. Discrete combinatorial circuits emerging in neural networks: A mechanism for rules of grammar in the human brain? Neural Networks. 2009;22(2):161–172. doi:10.1016/j.neunet.2009.01.009.

34. Pulvermüller F. Brain embodiment of syntax and grammar: Discrete combinatorial mechanisms spelt out in neuronal circuits. Brain and Language. 2010;112(3):167–179. doi:10.1016/j.bandl.2009.08.002.

35. Garagnani M, Lucchese G, Tomasello R, Wennekers T, Pulvermüller F. A Spiking Neurocomputational Model of High-Frequency Oscillatory Brain Responses to Words and Pseudowords. Frontiers in Computational Neuroscience. 2017;10. doi:10.3389/fncom.2016.00145.

36. Martin AE, Doumas LAA. A mechanism for the cortical computation of hierarchical linguistic structure. PLOS Biology. 2017;15(3):e2000663. doi:10.1371/journal.pbio.2000663.

37. de Kamps M. A generic approach to solving jump diffusion equations with applications to neural populations. arXiv preprint arXiv:13091654. 2013;.

38. Markram H. The Blue Brain Project. Nature Reviews Neuroscience. 2006;7(2):153–160. doi:10.1038/nrn1848.

39. Markram H. Seven challenges for neuroscience. Functional neurology. 2013;28(EPFL-REVIEW-216011):145–51.

40. Huyck CR, Passmore PJ. A review of cell assemblies. Biological Cybernetics. 2013;107(3):263–288. doi:10.1007/s00422-013-0555-5.

41. Perin R, Berger TK, Markram H. A synaptic organizing principle for cortical neuronal groups. Proceedings of the National Academy of Sciences. 2011;108(13):5419–5424. doi:10.1073/pnas.1016051108.

42. Edelman GM. Neural Darwinism: The theory of neuronal group selection. Basic Books; 1987.

43. Hebb DO. The organization of behavior: A neuropsychological theory. Psychology Press; 2005.

44. Destexhe A, Sejnowski TJ. The Wilson–Cowan model 36 years later. Biological Cybernetics. 2009;101(1):1–2. doi:10.1007/s00422-009-0328-3.

45. Frank VDV. Linking population dynamics and high-level cognition: Ambiguity resolution in a neural sentence processing model. Frontiers in Neuroinformatics. 2014;8. doi:10.3389/conf.fninf.2014.18.00055.

46. van der Velde F, de Kamps M. Learning of control in a neural architecture of grounded language processing. Cognitive Systems Research. 2010;11(1):93–107. doi:10.1016/j.cogsys.2008.08.007.

47. van der Velde F, de Kamps M. Development of a connection matrix for productive grounded cognition. In: 2011 IEEE International Conference on Development and Learning (ICDL). Institute of Electrical & Electronics Engineers (IEEE); 2011.Available from: http://dx.doi.org/10.1109/devlrn.2011.6037343.

48. van Dijk D, van der Velde F. A central pattern generator for controlling sequential activation in a neural architecture for sentence processing. Neurocomputing. 2015;170:128–140. doi:10.1016/j.neucom.2014.12.113.

49. de Kamps M, van der Velde F. Combinatorial structures and processing in Neural Blackboard Architectures. In: Pre-Proceedings of the Workshop on Cognitive Computation: Integrating Neural and Symbolic Approaches (CoCo@ NIPS 2015). Leeds; 2015.

50. de Kamps M. A Model for Delay Activity Without Recurrent Excitation. In: Artificial Neural Networks: Biological Inspirations – ICANN 2005. Springer Berlin Heidelberg; 2005. p. 229–234. Available from: https://doi.org/10.1007%2F11550822_37.

51. Nivre J. Dependency grammar and dependency parsing. MSI report. 2005;5133(1959):1–32.

52. Gazdar G. Phrase structure grammar. In: The nature of syntactic representation. Springer; 1982. p. 131–186.

53. Vagharchakian L, Dehaene-Lambertz G, Pallier C, Dehaene S. A Temporal Bottleneck in the Language Comprehension Network. Journal of Neuroscience. 2012;32(26):9089–9102. doi:10.1523/jneurosci.5685-11.2012.

54. Andor D, Alberti C, Weiss D, Severyn A, Presta A, Ganchev K, et al. Globally Normalized Transition-Based Neural Networks. In: Proceedings of the 54th Annual Meeting of the Association for Computational Linguistics (Volume 1: Long Papers). Association for Computational Linguistics (ACL); 2016.Available from: http://dx.doi.org/10.18653/v1/p16-1231.

55. Omurtag A, Knight BW, Sirovich L. On the simulation of large populations of neurons. Journal of computational neuroscience. 2000;8(1):51–63.

56. de Kamps M, Baier V, Drever J, Dietz M, Mösenlechner L, van der Velde F. The state of MIIND. Neural Networks. 2008;21(8):1164–1181. doi:10.1016/j.neunet.2008.07.006.

57. de Kamps M. A Generic Approach to Solving Jump Diffusion Equations with Applications to Neural Populations. arXiv preprint arXiv:13091654. 2013;.

58. Harrison D, De Kamps M. A New State of MIIND. In: Front. Neuroinform. Conference Abstract: 4th INCF Congress of Neuroinformatics. doi: 10.3389/conf. fninf. vol. 104; 2011.

59. Brette R, Rudolph M, Carnevale T, Hines M, Beeman D, Bower JM, et al. Simulation of networks of spiking neurons: a review of tools and strategies. Journal of computational neuroscience. 2007;23(3):349–398.

60. Brette R, Gerstner W. Adaptive exponential integrate-and-fire model as an effective description of neuronal activity. Journal of neurophysiology. 2005;94(5):3637–3642.

61. Benda J, Herz AVM. A Universal Model for Spike-Frequency Adaptation. Neural Computation. 2003;15(11):2523–2564. doi:10.1162/089976603322385063.

62. Benda J, Tabak J. Spike-Frequency Adaptation. In: Encyclopedia of Computational Neuroscience. Springer New York; 2014. p. 1–12. Available from: https://doi.org/10.1007%2F978-1-4614-7320-6_339-1.

63. Velde F, Kamps M. Ambiguity resolution in a Neural Blackboard Architecture for sentence structure. 2015;.

64. Brette R. Adaptive Exponential Integrate-and-Fire Model as an Effective Description of Neuronal Activity. Journal of Neurophysiology. 2005;94(5):3637–3642. doi:10.1152/jn.00686.2005.

65. Mazzoni A, Lindén H, Cuntz H, Lansner A, Panzeri S, Einevoll GT. Computing the Local Field Potential (LFP) from Integrate-and-Fire Network Models. PLOS Computational Biology. 2015;11(12):e1004584. doi:10.1371/journal.pcbi.1004584.

66. Hagen E, Dahmen D, Stavrinou M, Lindén H, Tetzlaff T, van Albada S, et al. Hybrid scheme for modeling local field potentials from point-neuron networks. BMC Neuroscience. 2015;16(Suppl 1):P67. doi:10.1186/1471-2202-16-s1-p67.

67. Wohrer A, Humphries MD, Machens CK. Population-wide distributions of neural activity during perceptual decision-making. Progress in Neurobiology. 2013;103:156–193. doi:10.1016/j.pneurobio.2012.09.004.

68. Kerr JND, Greenberg D, Helmchen F. From The Cover: Imaging input and output of neocortical networks in vivo. Proceedings of the National Academy of Sciences. 2005;102(39):14063–14068. doi:10.1073/pnas.0506029102.

69. Roxin A, Brunel N, Hansel D, Mongillo G, van Vreeswijk C. On the Distribution of Firing Rates in Networks of Cortical Neurons. Journal of Neuroscience. 2011;31(45):16217–16226. doi:10.1523/jneurosci.1677-11.2011.

70. London M, Schreibman A, Häusser M, Larkum ME, Segev I. The information efficacy of a synapse. Nat Neurosci. 2002;5(4):332–340. doi:10.1038/nn826.

71. Briggs F, Mangun GR, Usrey WM. Attention enhances synaptic efficacy and the signal-to-noise ratio in neural circuits. Nature. 2013;499(7459):476–480. doi:10.1038/nature12276.

72. Ostojic S. Two types of asynchronous activity in networks of excitatory and inhibitory spiking neurons. Nature Neuroscience. 2014;17(4):594–600. doi:10.1038/nn.3658.

73. nosuke Teramae J, Tsubo Y, Fukai T. Optimal spike-based communication in excitable networks with strong-sparse and weak-dense links. Sci Rep. 2012;2. doi:10.1038/srep00485.

74. Ray S, Maunsell JHR. Different Origins of Gamma Rhythm and High-Gamma Activity in Macaque Visual Cortex. PLoS Biology. 2011;9(4):e1000610. doi:10.1371/journal.pbio.1000610.

75. Manning JR, Jacobs J, Fried I, Kahana MJ. Broadband Shifts in Local Field Potential Power Spectra Are Correlated with Single-Neuron Spiking in Humans. Journal of Neuroscience. 2009;29(43):13613–13620. doi:10.1523/jneurosci.2041-09.2009.

76. Glover GH. Deconvolution of Impulse Response in Event-Related BOLD fMRI1. NeuroImage. 1999;9(4):416–429. doi:10.1006/nimg.1998.0419.

77. Friston KJ, Mechelli A, Turner R, Price CJ. Nonlinear Responses in fMRI: The Balloon Model Volterra Kernels, and Other Hemodynamics. NeuroImage. 2000;12(4):466–477. doi:10.1006/nimg.2000.0630.

78. Buxton RB, Uludağ K, Dubowitz DJ, Liu TT. Modeling the hemodynamic response to brain activation. NeuroImage. 2004;23:S220–S233. doi:10.1016/j.neuroimage.2004.07.013.

79. Waldorp L. Robust and Unbiased Variance of GLM Coefficients for Misspecified Autocorrelation and Hemodynamic Response Models in fMRI. International Journal of Biomedical Imaging. 2009;2009:1–11. doi:10.1155/2009/723912.

80. Turrigiano G. Too many cooks? Intrinsic and synaptic homeostatic mechanisms in cortical circuit refinement. Annual review of neuroscience. 2011;34:89–103.

81. Wolf F, Engelken R, Puelma-Touzel M, Weidinger JDF, Neef A. Dynamical models of cortical circuits. Current Opinion in Neurobiology. 2014;25:228–236. doi:10.1016/j.conb.2014.01.017.

82. Chomsky N. The Minimalist Program. The MIT Press; 2014. Available from: https://doi.org/10.7551%2Fmitpress%2F9780262527347.001.0001.